

Covalent Heterogenization of a Discrete Mn(II) Bis-Phen Complex by a Metal-Template/Metal-Exchange Method: An Epoxidation Catalyst with Enhanced Reactivity

Tracy J. Terry and T. Daniel P. Stack*

Department of Chemistry, Stanford University, Stanford, California 94305

Received June 8, 2007; E-mail: stack@stanford.edu

Abstract: Considerable attention has been devoted to the immobilization of discrete epoxidation catalysts onto solid supports due to the possible benefits of site isolation such as increased catalyst stability, catalyst recycling, and product separation. A synthetic metal-template/metal-exchange method to imprint a covalently attached bis-1,10-phenanthroline coordination environment onto high-surface area, mesoporous SBA-15 silica is reported herein along with the epoxidation reactivity once reloaded with manganese. Comparisons of this imprinted material with material synthesized by random grafting of the ligand show that the template method creates more reproducible, solution-like bis-1,10-phenanthroline coordination at a variety of ligand loadings. Olefin epoxidation with peracetic acid shows the imprinted manganese catalysts have improved product selectivity for epoxides, greater substrate scope, more efficient use of oxidant, and higher reactivity than their homogeneous or grafted analogues independent of ligand loading. The randomly grafted manganese catalysts, however, show reactivity that varies with ligand loading while the homogeneous analogue degrades trisubstituted olefins and produces *trans*-epoxide products from *cis*-olefins. Efficient recycling behavior of the templated catalysts is also possible.

Introduction

The epoxidation of olefins is of great interest due to the importance of epoxides in the manufacture of both bulk and fine chemicals. Epoxides serve as useful starting materials in the synthesis of a variety of functionalized organic compounds, as the epoxide ring reacts readily with a wide range of nucleophiles with high regioselectivity.^{1,2} The facile and regiospecific opening of terminal epoxides makes this class of epoxide particularly useful in the production of industrially important products such as surfactants, corrosion protection agents, and additives.³ While a wide range of homogeneous catalysts for olefin epoxidation exist,^{4–6} heterogeneous catalysts offer many potential advantages including easy product separation, long lifetime, and durability.⁷ For these reasons, much attention has focused on the development of heterogeneous catalysts for epoxidation reactions.^{7–12}

The first covalently attached epoxidation catalysts involved titanium embedded in silica supports¹³ and many variations on this theme of Lewis acid transition metals (Ti^{IV}, W^{VI}, Mo^{VI}, V^V, Cr^{VI}, Zr^{IV}) incorporated into silica supports have followed over the past 40 years.^{14–24} The high oxidation state of these metals, steric constraints of the zeolite supports, and long reaction times of these catalysts generally restrict the substrate scope to small, electron-rich olefins that form stable epoxides able to withstand the reaction conditions. Inspiration for many of the newer generation of heterogeneous epoxidation catalysts derives from recent advances in discrete homogeneous oxidation catalysts.

Immobilization of discrete metal complexes has led to several efficient and reusable epoxidation catalysts, which oxidize electron-rich olefins.^{8–11,25–27} Few of these materials, however, maintain high reactivity with terminal olefins and are even less

- (1) Smith, J. G. *Synthesis* **1984**, 629–656.
- (2) Schneider, C. *Synthesis-Stuttgart* **2006**, 3919–3944.
- (3) Weissmerl, K. *Industrial Organic Chemistry*, 3rd ed.; VCH: Weinheim, New York, 1997.
- (4) Lane, B. S.; Burgess, K. *Chem. Rev.* **2003**, *103*, 2457–2473.
- (5) McGarrigle, E. M.; Gilheany, D. G. *Chem. Rev.* **2005**, *105*, 1563–1602.
- (6) Colladon, M.; Scarso, A.; Sgarbossa, P.; Michelin, R. A.; Strukul, G. J. *Am. Chem. Soc.* **2007**, *129*, 7680–7689.
- (7) De Vos, D. E.; Sels, B. F.; Jacobs, P. A. *Immobilization of Homogeneous Oxidation Catalysts*; Academic Press, Inc.: 2001; Vol. 46.
- (8) De Vos, D. E.; Sels, B. F.; Jacobs, P. A. *Adv. Synth. Catal.* **2003**, *345*, 457–473.
- (9) De Vos, D. E.; Jacobs, P. A. *Catal. Today* **2000**, *57*, 105–114.
- (10) Kamata, K.; Yonehara, K.; Sumida, Y.; Yamaguchi, K.; Hikichi, S.; Mizuno, N. *Science* **2003**, *300*, 964–966.
- (11) De Vos, D. E.; Dams, M.; Sels, B. F.; Jacobs, P. A. *Chem. Rev.* **2002**, *102*, 3615–3640.
- (12) Terry, T. J.; Dubois, G.; Murphy, A.; Stack, T. D. P. *Angew. Chem., Int. Ed.* **2007**, *46*, 945–947.

- (13) Wulff, H. P.; Wattimena, F. US Patent 4367342, 1970.
- (14) Corma, A.; Garcia, H. *Chem. Rev.* **2002**, *102*, 38337–33892.
- (15) Tanev, P. T.; Chibwe, M.; Pinnavaia, T. J. *Nature* **1994**, *368*, 321–323.
- (16) Sato, T.; Dakka, J.; Sheldon, R. A. *J. Chem. Soc., Chem. Commun.* **1994**, 1887–1888.
- (17) Cambor, M. A.; Corma, A.; Martinez, A.; Perez Parienta, J. *J. Chem. Soc., Chem. Commun.* **1992**, *8*, 589–590.
- (18) Tozzola, G.; Mantegazza, M. A.; Ranghino, G.; Petrini, G.; Bordiga, S.; Ricchiardi, G.; Lamberti, C.; Zulian, R.; Zecchina, A. *J. Catal.* **1998**, *179*, 64–71.
- (19) Tuel, A.; Gontier, S.; Teissier, R. *J. Chem. Soc., Chem. Commun.* **1996**, 651–652.
- (20) Dongare, M. K.; Singh, P.; Moghe, P. P.; Ratnasamy, P. *Zeolites* **1991**, *11*, 690–693.
- (21) Singh, A.; Selvam, T. *J. Mol. Catal. A* **1996**, *113*, 489–497.
- (22) Rigutto, M. S.; Bekkum, H. V. *J. Mol. Catal.* **1993**, *81*, 77–98.
- (23) Ulagappan, N.; Rao, C. N. R. *J. Chem. Soc., Chem. Commun.* **1996**, *9*, 1047–1048.
- (24) Sels, B. F.; De Vos, D.; Jacobs, P. A. *Tetrahedron Lett.* **1996**, *37*, 8557–8560.

effective with more electron-deficient olefins such as α,β -unsaturated ketones and esters. The few heterogenized transition metal catalysts that epoxidize electron-deficient olefins, such as a covalently tethered Ru-porphyrin system,²⁴ have limitations including multiple reaction byproducts and a narrow substrate scope.^{25,26} No reported catalysts effectively combine high productivity and reusability with simple oxidants and a wide substrate scope.

[Mn^{II}(phen)₂]X₂, in which X is a weakly coordinating anion and phen is 1,10-phenanthroline, was recently reported as a highly active, homogeneous, electrophilic epoxidation catalyst with peracetic acid (PAA) as the oxidant.²⁸ The high reactivity, broad substrate scope, simple oxidant, and convenient reaction conditions make [Mn^{II}(phen)₂]²⁺ and PAA an attractive epoxidation system. While the [Mn^{II}(phen)₂]²⁺/PAA system is efficient with many unfunctionalized disubstituted and α -olefins as well as α,β -unsaturated ketones and esters, limitations exist possibly related to radical processes and/or side reactions. [Mn^{II}(phen)₂]²⁺ requires 2 equiv of PAA per alkene at low catalyst loading (<0.05 mol %) for high conversions, degrades electron-rich tri- and tetrasubstituted olefins, and *cis*-olefins are partially isomerized yielding *trans*-epoxide products. As reactivity studies suggest that the active catalyst is monomeric,²⁹ immobilized [Mn^{II}(phen)₂]²⁺ was targeted for further study. We now report improvement in the catalytic activity of [Mn^{II}(phen)₂]²⁺ by covalently attaching this species onto a porous SBA-15 silica support.

Recent advances in the heterogenization of discrete homogeneous catalysts predominantly employ tethering of single, multidentate ligands such as a porphyrin, salen, or 1,4,7-triazacyclononane, which provide the requisite metal coordination for catalytic activity.^{7,8} Random grafting of such complexes onto a support ensures the retention of the homogeneous coordination sphere and catalytic reactivity. Reports of immobilized coordination environments for a single metal created from several independent ligands, such as [Mn^{II}(phen)₂]²⁺, are limited. Immobilization into zeolites without covalent attachment of [Mn^{II}(bpy)₂]²⁺ (bpy = bipyridine) significantly improved the catalytic epoxidation reactivity with H₂O₂.³⁰ This encapsulation strategy is suggested to site-isolate [Mn^{II}(bpy)₂]²⁺, preventing formation of polynuclear μ -oxo or μ -hydroxo complexes that efficiently disproportionate H₂O₂.³¹ Covalent imprinting of coordination sites composed of several independent ligands is also limited with the greatest success in the area of organic supports.³² Borovik et al. report a particularly interesting example of a covalently attached multiligand coordination complex for nitric oxide delivery in which both the metalated porphyrin and the axial ligand are maintained upon immobilization.^{33,34}

A significant challenge in grafting organic molecules onto porous materials is controlling their concentration and distribu-

tion.³⁵ To construct coordination sites with two tetherable 1,10-phenanthroline ligands, hereafter referred to as a bis-phen coordination, we have used a metal-template/metal-exchange method at low surface loadings to ensure correlated pairs of covalently attached phenanthroline ligands. These templated materials loaded with manganese show enhanced epoxidation reactivity with PAA over a range of ligand loadings compared to materials prepared with randomly grafted phenanthroline ligands. The latter are less selective epoxidation catalysts with variable reactivity dependent on loading. A similar templating approach led to an imprinted ferrous bis-phen species, which possesses a coordination that is thermodynamically unstable in a homogeneous solution. These iron materials were shown to be active epoxidation catalysts¹² but do not approach the efficiency, selectivity, substrate scope, or recyclability achieved with the manganese catalyst materials reported herein.

Experimental Section

General Considerations. The following chemicals were used as received: P123 (Aldrich), tetraethyl orthosilicate (TEOS) (Aldrich), thionyl chloride (SOCl₂) (Fluka), 3-mercaptopropyl triethoxysilane (Gelest, Inc.), pentanes (Aldrich), sodium diethyldithiocarbamate (Et₂NCS₂Na) (Acros), anhydrous acetonitrile (MeCN) (Aldrich), acetic acid (J. T. Baker), 50% H₂O₂ (EMD), and methanol (MeOH) (VWR). Anhydrous tetrahydrofuran (THF) was obtained from a packed bed solvent purification system using an alumina column. Amberlite IR-120 resin (Fluka) was rinsed with acetic acid before use. All syntheses were performed under a N₂ atmosphere using standard Schlenk line techniques unless otherwise specified. NMR spectra were obtained on an Inova 300 MHz NMR spectrometer with a Varian Inova console using Solaris 2.7 software.

Synthesis of SBA-15. Micelle templated silica SBA-15 was prepared according to the literature using a triblock copolymer as the surfactant template.³⁶ In a typical synthesis, 12 g of P123 was dissolved in 90 mL of distilled water and 360 g of 2 M HCl with stirring at 40 °C. Once the solution was visibly homogeneous, 27 mL of TEOS were added dropwise to the solution over 1 min. The mixture was stirred at 40 °C for 24 h, transferred to a glass pressure vessel, and heated in an oven at 100 °C for 24 h. The resulting material was filtered with deionized water and ethanol, air-dried, and calcined at 550 °C in air for 5 h to remove the surfactant template.

Ligand Syntheses. Ethyl 4-(3-(triethoxysilyl)propylthio)-1,10-phenanthroline-3-carboxylate, **1^H** (Scheme 1), was prepared by adding 6 g of 4-hydroxy-[1,10]phenanthroline-3-carboxylic acid ethyl ester³⁷ to 20 mL of SOCl₂ and a catalytic amount of DMF for 1 h at 85 °C. After cooling, the SOCl₂ was removed under vacuum and the product separated as a solid from a mixture of 500 mL of 10% K₂CO₃ and 500 mL of ethyl acetate to give 5.3 g of crude 4-chloro-[1,10]phenanthroline-3-carboxylic acid ethyl ester. This material was recrystallized from hot heptanes (75% yield). The product was stirred with 1.4 equiv of 3-mercaptopropyl triethoxysilane and K₂CO₃ in 100 mL of anhydrous THF under N₂ for 12 h at 65 °C. The mixture was cooled and filtered, and the THF was removed under vacuum to give a yellow oil. Dissolution of the oil in pentane followed by cooling to -115 °C separated **1^H** in a pure form. ¹H NMR (300 MHz, CDCl₃, δ): 9.20 (s, 1H), 9.17 (d/d, 1H), 8.59 (d, 1H), 8.23 (d/d, 1H), 7.86 (d, 1H), 7.63 (d/d, 1H), 4.74 (m, 2H), 3.67 (q, 6H), 2.96 (t, 2H), 1.61 (m, 2H), 1.43 (t, 3H), 1.08 (t, 9H), 0.64 (m, 2H). HRMS-EI⁺ [M⁺], calculated *m/z* = 488.1801, found *m/z* = 488.1787. Anal. Calcd for C₂₄H₃₂N₂O₅SSi: C, 58.99; H, 6.60; N, 5.73; O, 16.37; S, 6.56. Found: C, 57.62; H, 6.31; N, 5.72; S, 5.92. The phen derivative **2** was prepared in a similar manner

(25) Yu, X.-Q.; Huang, J.-S.; Yu, W.-Y.; Che, C.-M. *J. Am. Chem. Soc.* **2000**, *122*, 5337–5342.

(26) Sasidharan, M.; Wu, P.; Tatsumi, T. *J. Catal.* **2002**, *205*, 332–338.

(27) Holbach, M.; Weck, M. *J. Org. Chem.* **2006**, *71*, 1825–1836.

(28) Murphy, A.; Pace, A.; Stack, T. D. P. *Org. Lett.* **2004**, *6*, 3119–3122.

(29) Murphy, A.; Stack, T. D. P. *J. Mol. Catal. A* **2006**, *251*, 78–88.

(30) Knopsgrits, P. P.; De Vos, D.; Thibaultstarzyk, F.; Jacobs, P. A. *Nature* **1994**, *369*, 543–546.

(31) Okawa, H.; Sakiyama, H. *Pure Appl. Chem.* **1995**, *67*, 273–280.

(32) Becker, J. J.; Gagne, M. R. *Acc. Chem. Res.* **2004**, *37*, 798–804.

(33) Welbes, L. L.; Borovik, A. S. *Acc. Chem. Res.* **2005**, *38*, 765–774.

(34) Mitchell-Koch, J. T.; Padden, K. M.; Borovik, A. S. *J. Polym. Sci., Part A: Polym. Chem.* **2006**, *44*, 2282–2292.

(35) Corriu, R. J. P.; Mehdi, A.; Reye, C.; Thieuleux, C. *Chem. Mater.* **2003**, *16*, 159–166.

(36) Zhao, D. Y.; Huo, Q. S.; Feng, J. L.; Chmelka, B. F.; Stucky, G. D. *J. Am. Chem. Soc.* **1998**, *120*, 6024–6036.

(37) Markees, D. G. *Helv. Chim. Acta* **1983**, *66*, 620–626.

in 70% overall yield. ^1H NMR (300 MHz, CDCl_3 , δ): 9.25 (s, 1H), 9.21 (d/d, 1H), 8.66 (d, 1H), 8.27 (d/d, 1H), 7.90 (d, 1H), 7.67 (d/d, 1H), 4.51 (m, 2H), 3.50 (m, 1H), 1.46 (t, 3H), 1.23 (d, 6H). HRMS- EI^+ [M^+], calculated $m/z = 326.1089$, found $m/z = 326.1084$.

Templating and Cu^{I} Removal Procedure. In a typical synthesis, $\mathbf{1}^{\text{H}}$ (500 mg, 1.02 mmol) was combined with 190 mg (0.51 mmol) of $[\text{Cu}(\text{CH}_3\text{CN})_4]\text{PF}_6$ in a 200 mL Schlenk flask under N_2 . Approximately 150 mL of MeCN were added to form a deep brown solution before the addition of 7.5 g of SBA-15. The solution was stirred overnight at 70 °C and filtered in air to give $\text{Cu}^{\text{I}}\mathbf{T}$ (Scheme 1) with a loading of 0.11 mmol g^{-1} of $\mathbf{1}^{\text{C}}$ ($\mathbf{1}^{\text{C}} = \mathbf{1}^{\text{H}}$ after covalent attachment to the silica surface). Approximately 75% of $\mathbf{1}^{\text{H}}$ was immobilized to the silica by this procedure as determined by sulfur analysis; the ligand/copper ratio was 2.2(1):1. Removal of Cu^{I} from $\text{Cu}^{\text{I}}\mathbf{T}$ was accomplished with several metal complexing agents including EDTA or sodium diethyldithiocarbamate. In a typical procedure, 7 g of $\text{Cu}^{\text{I}}\mathbf{T}$ was stirred with 300 mL of 0.1 M sodium diethyldithiocarbamate in CH_3OH for 2 h, filtered, and rinsed with CH_3OH and acetone. This process was repeated three times to give the bis-phen templated SBA-15, \mathbf{T} , with less than 0.002 mmol g^{-1} Cu.

Grafting Procedure. In a typical synthesis of the randomly grafted $\mathbf{1}^{\text{H}}$ in SBA-15 to give \mathbf{G} , 810 mg (1.65 mmol) of $\mathbf{1}^{\text{H}}$ and 2 g of SBA-15 were stirred overnight in 100 mL of MeCN in a 200 mL Schlenk flask under N_2 at 70 °C. Filtering gave \mathbf{G} with a loading of 0.10 mmol g^{-1} $\mathbf{1}^{\text{C}}$; only ca. 15% of $\mathbf{1}^{\text{H}}$ used in the reaction was covalently attached to the silica as determined by sulfur analysis, but the unreacted $\mathbf{1}^{\text{H}}$ in the filtrate could be reused.

Grafting Procedure for High Ligand Density Materials. In a typical synthesis of the high ligand density materials, 1.60 g (3.30 mmol) of $\mathbf{1}^{\text{H}}$ and 0.35 g of SBA-15 were stirred for 48 h in 100 mL of MeCN in a 200 mL Schlenk flask under N_2 at 70 °C. Filtering gave \mathbf{G} with a loading of 0.91 mmol g^{-1} $\mathbf{1}^{\text{C}}$.

Metalation Procedure. Approximately 0.2 mmol of $[\text{M}(\text{CF}_3\text{SO}_3)_2]$ ($\text{M} = \text{Mn}^{\text{II}}$ or Cu^{II}) per gram of material (2 equiv M^{II} per $\mathbf{1}^{\text{C}}$) were stirred in CH_3OH overnight before filtering. To remove any weakly coordinated metal, the metalated materials were stirred in refluxing CH_3OH for 2 h, filtered and washed with copious amounts of CH_3OH .

Peracetic Acid Preparation. In a 20 mL Nalgene bottle equipped with a magnetic stir bar, 50% hydrogen peroxide (1.75 mL) was added to a slurry of acetic acid (15 g) and Amberlite IR-120 (0.5 g). The slurry was stirred overnight in an ice bath and filtered through a glass microfiber filter (1.2 μm pores). The PAA mol % was determined by integration of the ^{13}C NMR peaks of acetic acid and peracetic acid in D_2O or by a standard titration.³⁸ This preparative method yields ca. 8 mol % PAA solutions, which were stored at -20 °C in a Nalgene bottle and used within a month of synthesis.

Representative Epoxidation Conditions. In a representative reaction, a mixture of 85 μL of MeCN, 5 mg of $\text{Mn}^{\text{II}}\mathbf{T}$ (0.11 mmol g^{-1} $\mathbf{1}^{\text{C}}$, 0.30 μmol Mn, 0.5 mol %), 8 μL of vinylcyclohexane (58 μmol), and 1 μL of *n*-decane (internal standard, 0.51 μmol) was prepared in a 10 mL test tube at 2 °C with a stir bar. 66 μL of an 8% PAA (1.5 equiv) were added dropwise over 2 min. The reaction was stirred for an additional 8 min, diluted with diethyl ether, and filtered through a basic alumina plug in a glass pipet. GC analysis of the solution provided the substrate conversion and product yield relative to the internal standard. The epoxide product was identified by ^1H NMR and by a comparison of the GC retention time to an authentic sample.

Recycling Conditions. Each trial was setup as described above (0.5 mol % Mn, 0.4 M vinylcyclohexane, MeCN, 1.5 equiv 8% PAA, 2 °C) except that 100 mg of $\text{Mn}^{\text{II}}\mathbf{T}$ or $\text{Mn}^{\text{II}}\mathbf{G}$ were used initially in a 20 mL scintillation vial. The PAA, prepared on the day of the experiment, was added dropwise over ca. 5 min to ensure that the heat of the reaction was efficiently dissipated. After 10 min, the catalyst material was filtered and an aliquot of the solution was analyzed by

GC. The catalyst material was washed with acetone, and after drying in air, 10 mg were reserved for sulfur and manganese ICP analysis. The remaining catalyst used in subsequent trials was assumed to fully retain all of the initial manganese.

Inductively Coupled Plasma Atomic Emission Spectroscopy (ICP). Each 10–20 mg sample of vacuum-dried material was dissolved in ca. 1 mL of boiling 5% KOH and diluted to 10 mL with deionized (DI) water. A 5 mL aliquot was acidified with 1 mL of concentrated HNO_3 before dilution to 10 mL with DI water. Each basic solution was filtered through a 0.45 μm polytetrafluoroethylene filter and submitted for sulfur analysis, while each acidic solution was filtered through a 0.45 μm polyethersulfone filter and submitted for metal analysis. ICP analysis was conducted on a TJA IRIS Advantage 1000 Radial ICAP spectrometer with a solid-state CID detector.

Porosimetry Analysis. Dinitrogen adsorption and desorption isotherms at -196 °C were measured using a Micromeritics ASAP 2010 porosimeter. Surface area calculations were conducted using the BET (Brunauer–Emmett–Teller) method,³⁹ and the pore diameter calculations were conducted using the BJH (Barrett–Joyner–Halenda) method.⁴⁰

EPR Analysis. EPR spectra were collected on a Bruker EMX spectrometer with a Bruker ER 041XG QR microwave bridge and ER 4102ST cavity. For solid samples, ca. 6 mg of each material was suspended in ca. 0.1 mL of solvent and cooled to -196 °C. Similar spectra were obtained in ethanol or a 2:1 mixture of 2-methyltetrahydrofuran and propionitrile. For homogeneous samples, ca. 0.5 mM samples in a 2:1 mixture of 2-methyltetrahydrofuran and propionitrile were cooled to -196 °C. The Mn^{II} complexes $[\text{Mn}^{\text{II}}(1,10\text{-phenanthroline})]^{2+}$, $[\text{Mn}^{\text{II}}(1,10\text{-phenanthroline})_2]^{2+}$, and $[\text{Mn}^{\text{II}}(1,10\text{-phenanthroline})_3]^{2+}$ were prepared in situ by mixing of appropriate molar quantities of $\text{Mn}^{\text{II}}(\text{CF}_3\text{SO}_3)_2$ and 1,10-phenanthroline while $[\text{Cu}^{\text{II}}(\mathbf{2})_2](\text{CF}_3\text{SO}_3)_2$ was isolated before sample preparation $\{[\text{Cu}^{\text{II}}(\mathbf{2})_2](\text{CF}_3\text{SO}_3)_2$: MS- ES^+ [M^{2+}], calculated $m/z = 357.6$, found $m/z = 358.0$; MS- ES^+ [M^+], calculated $m/z = 864.1$, found $m/z = 864.4$ }. Simulations were performed using Simfonia software.

Results

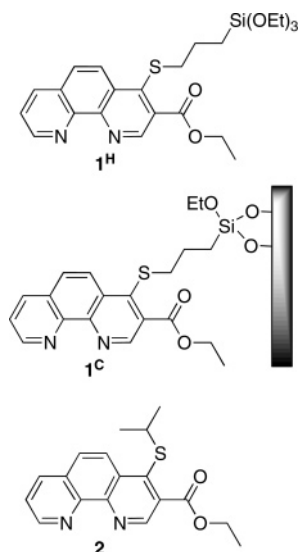
Derivatization of the 1,10-phenanthroline ligand backbone was necessary to allow immobilization and quantification of the ligand. The propyltrialkoxysilane moiety allows for covalent attachment of $\mathbf{1}^{\text{H}}$ to the silica surface while the sulfur atom, purposefully incorporated, allows quantitative comparisons of the covalently attached ligand to metal and counteranion content from a single digested sample by Inductively Coupled Plasma spectroscopy (ICP). Ligand $\mathbf{2}$ and $[\text{Mn}^{\text{II}}(\mathbf{2})_2](\text{CF}_3\text{SO}_3)_2$ provide a homogeneous comparison to the spectroscopic and reactivity properties of the heterogenized ligand and catalysts.

Two methods of covalent attachment of $\mathbf{1}^{\text{H}}$ on the SBA-15 silica were investigated: random grafting and metal-templating to create materials \mathbf{G} and \mathbf{T} , respectively (Scheme 1). Grafting involved random attachment of $\mathbf{1}^{\text{H}}$ to the support surface in the absence of any transition metal to form an anticipated uncorrelated distribution of covalently attached ligands, $\mathbf{1}^{\text{C}}$. Metalation of this material with 2 equiv of $[\text{Mn}^{\text{II}}(\text{CF}_3\text{SO}_3)_2]$ per $\mathbf{1}^{\text{C}}$ in methanol gave $\text{Mn}^{\text{II}}\mathbf{G}$, after removal of any weakly associated manganese with methanol washings. Metal-templating involved an initial formation of an air stable $[\text{Cu}^{\text{I}}(\mathbf{1}^{\text{H}})_2]^+$ complex followed by covalent attachment to the SBA-15 silica to yield $\text{Cu}^{\text{I}}\mathbf{T}$. Removal of the copper gave \mathbf{T} , with an anticipated correlated distribution of pairs of covalently attached ligands.

(39) Brunauer, S.; Emmett, P. H.; Teller, E. *J. Am. Chem. Soc.* **1938**, *60*, 309–319.

(40) Barrett, E. P.; Joyner, L. G.; Halenda, P. P. *J. Am. Chem. Soc.* **1951**, *73*, 373–380.

(38) Dixon, W. T. *Talanta* **1966**, *13*, 1199–1200.



Metalation of **T** with $[\text{Mn}^{\text{II}}(\text{CF}_3\text{SO}_3)_2]$ gave $\text{Mn}^{\text{II}}\text{T}$. The catalytic epoxidation reactivity of $\text{Mn}^{\text{II}}\text{T}$ and $\text{Mn}^{\text{II}}\text{G}$ are compared herein, each with several concentrations of covalently attached phenanthroline ligands.

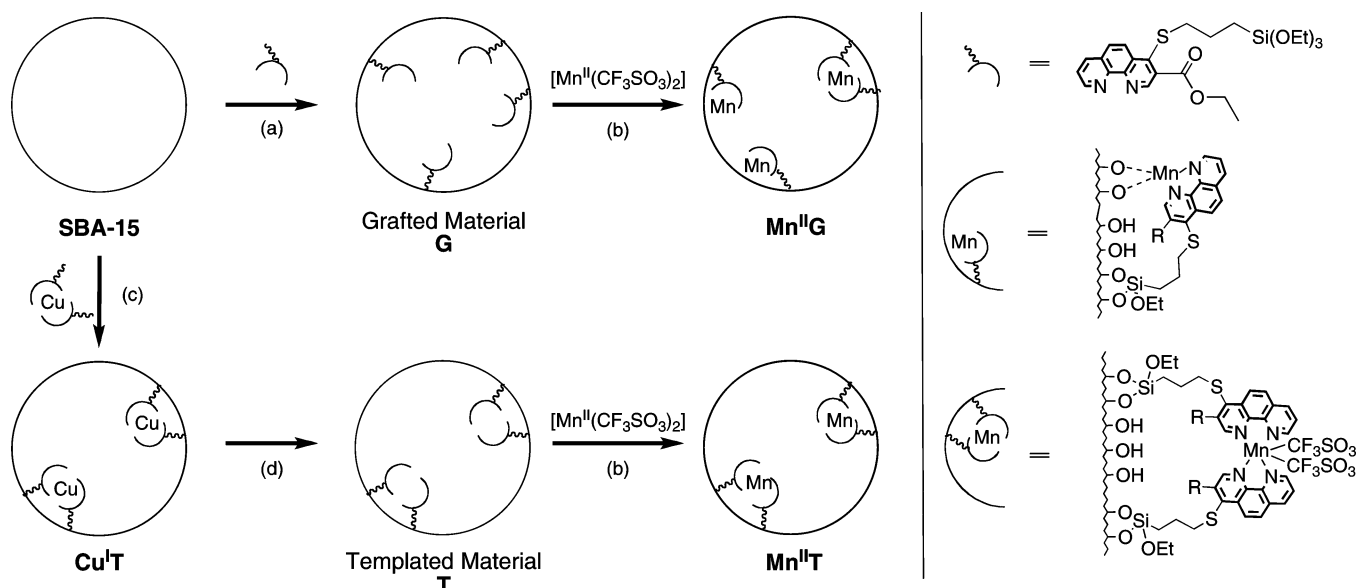
Material Stability. SBA-15 is a readily synthesized, micelle-templated, high surface area, mesoporous silica that is stable to acidic conditions.⁴¹ The material used in this investigation had an average pore diameter of ca. 65 Å and an average surface area of ca. 650 m² g⁻¹ and was found to be stable to the PAA oxidation conditions used herein.¹² The surface area and pore diameter were determined after the material was subjected to various reaction conditions employed during the synthesis, modification, and catalytic epoxidation trials.⁴² Only basic solutions of EDTA significantly altered the pore structure and surface area of the support; exposure of the materials for 1 h to a 0.1 M EDTA at pH 5 and 8 resulted in a 17% decrease and 70% increase, respectively, in the surface area. Further analysis of the SBA-15 stability at both higher pH (neat pyridine) and

lower pH (1 M nitric acid) over 4 h demonstrated the overall stability of the material under acidic conditions, as the former increased the surface area by 42%, while the latter resulted in only a 4% change. The preferred demetalation procedure of 4 h at ambient conditions with a 0.1 M aqueous solution of sodium diethyldithiocarbamate only resulted in a small change in the surface area (+3%).

Material Analysis. A maximum loading of 0.9 mmol g⁻¹ **1C** could be achieved under random grafting conditions using a ca. 10-fold excess of **1H** over extended reaction times (48 h) at 70 °C in acetonitrile. This loading is close to the standard full loading of ca. 1.2 mmol g⁻¹ of an alkyl triethoxysilane on mesoporous silica with a surface area of ca. 600 m² g⁻¹.⁴³ At 1 mmol g⁻¹ loadings, however, the ligands are sufficiently close to allow a single metal center to be ligated by two **1C**.⁴² Assuming a tether length of ca. 10 Å for **1C**,⁴² the distance between the silicon atom and the center of the two coordinating nitrogen atoms of the ligand in an extended alkyl chain conformation, an average separation of ca. 20 Å is needed to achieve site isolation of a single **1C** on the surface. Such site isolation of **1C** on a 600 m² g⁻¹ material requires a ligand loading of no more than ca. 0.30 mmol g⁻¹. Significantly more efficient and selective reactivity and consistent material synthesis (vide infra) are possible at the lower ligand loadings of 0.3, 0.1, and 0.025 mmol g⁻¹ of **1C**.

Copper removal and reloading from the templated materials was a fully reversible process as assessed by copper analysis (Table 1, entries 3–5). Manganese uptake by the templated materials at various **1C** loadings (0.30, 0.11, and 0.025 mmol g⁻¹) consistently yielded ca. 2:1 ratios of **1C**/Mn^{II} (Table 1, entries 6–8). By contrast, the manganese uptake by randomly grafted materials, at various **1C** loadings (0.90, 0.10, and 0.025 mmol g⁻¹) yielded materials with less predictable ligand to manganese ratios. At low loadings, a **1C**/metal ratio near 1:1 was observed consistently for $\text{Mn}^{\text{II}}\text{G}$ and $\text{Cu}^{\text{II}}\text{G}$ (Table 1, entries 11–13). Control experiments indicate that the unmodi-

Scheme 1. Schematic Representation of the Covalent Attachment of **1H** to the SBA-15 Silica via Random Grafting and Metal-Templating Methods To Form $\text{Mn}^{\text{II}}\text{G}$ and $\text{Mn}^{\text{II}}\text{T}$, Respectively^a



^a (a) Random grafting of **1H**, (b) metalation with an excess of $[\text{Mn}^{\text{II}}(\text{CF}_3\text{SO}_3)_2]$ per **1C** followed by washing with CH_3OH , (c) formation of $[\text{Cu}^{\text{II}}(\text{1H})_2]^+$ followed by covalent attachment, (d) demetalation with $\text{Et}_2\text{NCS}_2\text{Na}$.

Table 1. Metal and Ligand Content in Materials from ICP Analysis

entry	material	ligand 1 ^c (mmol g ⁻¹) ± 0.01 ^a	metal (mmol g ⁻¹) ± 0.002 ^a	1 ^c /metal
1	SBA-15 ^b	0.00	0.001	
2	SBA-15 ^c	0.00	0.005	
3	Cu ^{II} T	0.11	0.051	2.2
4	T	0.11	0.001	
5	Cu ^{II} T	0.11	0.052	2.1
6	Mn ^{II} T	0.30	0.14	2.1
7	Mn ^{II} T	0.11	0.055	2.0
8	Mn ^{II} T	0.025	0.013	1.9
9	G	0.10	0.001	
10	Mn ^{II} G	0.90	0.10	9.0
11	Mn ^{II} G	0.10	0.085	1.2
12	Mn ^{II} G	0.025	0.028	1.1
13	Cu ^{II} G	0.10	0.057	1.7

^a Standard deviations determined from a minimum of three ICP measurements on the same material. ^b Manganese concentration in unmodified SBA-15. ^c Manganese concentration in unmodified SBA-15 after metalation with [Mn^{II}(CF₃SO₃)₂] and washing with CH₃OH.

fied silica retains no appreciable metal after the metalation/washing conditions (Table 1, entry 2).

X-band EPR spectroscopy at -196 °C of the all the Mn^{II} materials yielded nearly identical spectra. The spectra of Mn^{II}T, Mn^{II}G, and the homogeneous complexes [Mn^{II}(2)₁]²⁺, [Mn^{II}(2)₂]²⁺, and [Mn^{II}(2)₃]²⁺ each displayed a six-line, *g* ≈ 2 signal typical of a high-spin Mn^{II} species.⁴² The X-band EPR spectra of the Cu^{II} materials were a more sensitive probe of the coordination environments. The spectra of [Cu^{II}(2)₂]²⁺, Cu^{II}G, and Cu^{II}T¹² all displayed characteristic mononuclear axial signals consistent with a d_{x²-y²} electronic ground state. The spectra of [Cu^{II}(2)₂](CF₃SO₃)₂ and Cu^{II}T are comparable with similar signals at *g*_⊥ = 2.06 and *g*_∥ = 2.270, while Cu^{II}G shows a significant shift of the parallel feature to lower field (*g*_∥ = 2.295). None of the EPR spectra of Cu^{II}G and Cu^{II}T at 0.1 mmol g⁻¹ 1^c shifted with a change in solvent conditions from ethanol to 2-methyltetrahydrofuran/propionitrile (2:1). The EPR spectra of Cu^{II}T and [Cu^{II}(2)₂](CF₃SO₃)₂ were not affected by the addition of 2 equiv of (*n*-Bu₄N)Cl per copper in 2-methyltetrahydrofuran/propionitrile (2:1), while a second signal (*g*_∥ = 2.255) appeared in the EPR spectrum of Cu^{II}G (Figure 1).

Substrate Scope and Epoxide Selectivity. Mn^{II}T, Mn^{II}G, and [Mn^{II}(2)₂]²⁺ were investigated initially for their ability to epoxidize vinylcyclohexane (Table 2), and Mn^{II}T was found to be the most reactive and selective of all the catalysts. The high reactivity and epoxide selectivity of Mn^{II}T is constant at each ligand loading of 1^c, while the lower epoxide selectivity with Mn^{II}G parallels that of the homogeneous system if only 1 equiv of 2 or 1,10-phenanthroline (phen) per Mn^{II} is used in the catalyst preparation.

The reaction rate with Mn^{II}T is ca. 5 × faster than that with Mn^{II}G at a similar catalyst loading while maintaining higher selectivity for the epoxide (Figure 2). The reaction profiles reported with 1-octene parallel the reactivity presented in Table 2 with vinylcyclohexane.

Mn^{II}T functions with a wider range of substrates than the homogeneous catalysts and requires less oxidant for higher

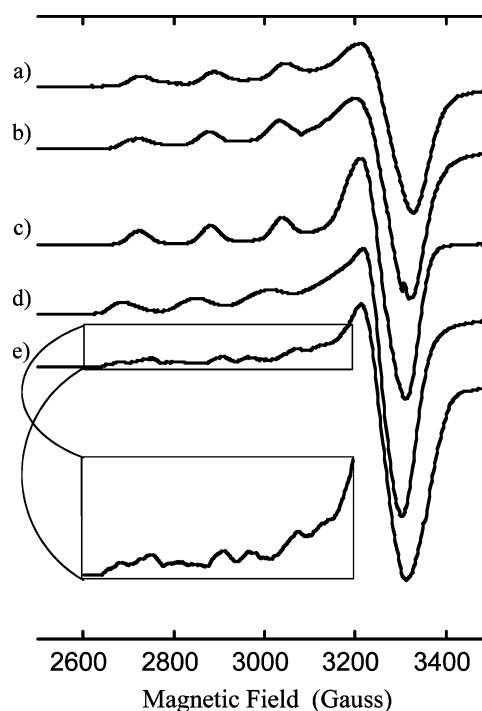


Figure 1. X-band EPR signals in 2-methyltetrahydrofuran/propionitrile (2/1) at -196 °C of (a) Cu^{II}T (0.1 mmol g⁻¹ 1^c), (b) Cu^{II}T (0.1 mmol g⁻¹ 1^c) with 2 equiv of (*n*-Bu₄N)Cl per copper, (c) [Cu^{II}(2)₂](OTf)₂ (1 mM), (d) Cu^{II}G (0.08 mmol g⁻¹ 1^c), and (e) Cu^{II}G (0.08 mmol g⁻¹ 1^c) with 2 equiv of (*n*-Bu₄N)Cl per copper.

Table 2. Epoxidation Reactivity of Mn^{II} Catalysts with Vinylcyclohexane^a

catalyst	yield (±3%) ^{b,d}	selectivity (±3%) ^{b,d}
[Mn ^{II} (phen) ₂] ²⁺ ^e	95	95
[Mn ^{II} (phen) ₁] ²⁺ ^e	72	72
[Mn ^{II} (2) ₂] ²⁺ ^e	80	85
[Mn ^{II} (2) ₁] ²⁺ ^e	73	73
Mn ^{II} T (0.30 mmol g ⁻¹ 1 ^c)	97	97
Mn ^{II} T (0.11 mmol g ⁻¹ 1 ^c)	98	98
Mn ^{II} T (0.025 mmol g ⁻¹ 1 ^c)	98	98
Mn ^{II} G (0.90 mmol g ⁻¹ 1 ^c)	80	84
Mn ^{II} G (0.11 mmol g ⁻¹ 1 ^c)	83	83
Mn ^{II} G (0.025 mmol g ⁻¹ 1 ^c)	72	72

^a 0.5 mol % Mn, 0.4 M vinylcyclohexane, 2 °C, 10 min, MeCN; 1.8 equiv of PAA were used with the homogeneous catalysts, and 1.5 equiv of PAA were used with the immobilized catalysts. Each catalyst converts >95% of the vinylcyclohexane. ^b Epoxide yield relative to an internal standard as determined by GC. ^c Epoxide selectivity indicates the percentage of vinylcyclohexane that is converted to epoxide. ^d Average of five reactions; the results were reproducible with different preparations of catalysts at the same ligand loadings. ^e The homogeneous catalysts were prepared in situ.

epoxide selectivities (Table 3). Since reasonable epoxide yields and selectivities are obtained for [Mn^{II}(2)₂]²⁺ with disubstituted and terminal olefins (Table 3, entries 3–11), the advantages of covalent attachment of the catalysts to the silica are most evident with the trisubstituted electron-rich olefins (Table 3, entry 1) and the more electron-deficient olefins (Table 3, entries 12–16). [Mn^{II}(2)₂]²⁺ fully oxidizes trisubstituted olefins without appreciable epoxide production and isomerizes ca. 5% of internal *cis*-olefins to the *trans*-epoxide products. By contrast, Mn^{II}T provides nearly a quantitative yield of trisubstituted epoxide and

(41) Cassiers, K.; Linssen, T.; Mathieu, M.; Benjelloun, M.; Schrijnemakers, K.; Van Der Voort, P.; Cool, P.; Vansant, E. F. *Chem. Mater.* **2002**, *14*, 2317–2324.

(42) See Supporting Information.

(43) Zhao, X. S.; Lu, G. Q.; Whittaker, A. K.; Millar, G. J.; Xhu, H. Y. *J. Phys. Chem. B* **1997**, *101*, 6525–6531.

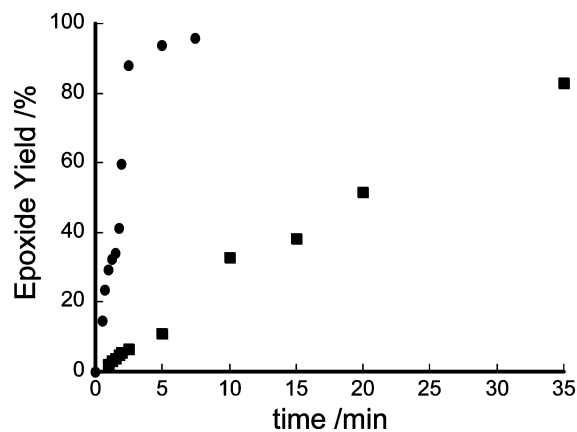


Figure 2. Conversion of 1-octene to 1,2-epoxyoctane by $\text{Mn}^{\text{II}}\text{T}$ (●) ($0.11 \text{ mmol g}^{-1} \mathbf{1}^{\text{C}}$) and $\text{Mn}^{\text{II}}\text{G}$ (■) ($0.10 \text{ mmol g}^{-1} \mathbf{1}^{\text{C}}$) in MeCN at 2°C with 1.5 equiv of PAA.

no measurable isomerization of *cis*-olefins (Table 3, entries 1 and 2). $\text{Mn}^{\text{II}}\text{G}$ is also more selective than the homogeneous catalysts with ca. 90% epoxide yields of trisubstituted olefins, yet with ca. 5% isomerization of *cis*-2-heptene to its *trans*-epoxide product. $\text{Mn}^{\text{II}}\text{T}$ mediates efficiently epoxidation of α,β -unsaturated ketones and esters, whereas the conversion of electron-deficient olefins is incomplete with $[\text{Mn}^{\text{II}}(\mathbf{2})_2]^{2+}$ at 0.5 mol % Mn and 1.8 equiv of PAA per olefin. Increasing the number of equivalents of PAA with $[\text{Mn}^{\text{II}}(\mathbf{2})_2]^{2+}$ did not improve the epoxide yields. In the cases of highly electron-deficient olefins that were not fully epoxidized with 1.5 equiv of PAA per olefin and $\text{Mn}^{\text{II}}\text{T}$, higher yields and selectivities were possible by the addition of more oxidant (Table 3, entries 13–16).

Chemoselectivity. The electrophilic chemoselectivity of these Mn^{II} oxidants is evident from the reactivity with ethyl sorbate (Table 3, entry 14); the more electron-rich olefin is oxidized preferentially yielding the 4,5-monoepoxide product before significant formation of the diepoxide product. Intermolecular competition experiments with 1-octene and allyl acetate, at low conversions, further highlight the electrophilic nature of the active oxidants (Table 4). The bis-coordinated homogeneous catalysts, $[\text{Mn}^{\text{II}}(\text{phen})_2]^{2+}$ and $[\text{Mn}^{\text{II}}(\mathbf{2})_2]^{2+}$, show the highest selectivity for the more electron-rich 1-octene substrate, while the monoligated Mn^{II} complexes, $[\text{Mn}^{\text{II}}(\text{phen})_1]^{2+}$ and $[\text{Mn}^{\text{II}}(\mathbf{2})_1]^{2+}$, exhibit lesser chemoselectivity in the epoxidation reaction. The chemoselectivity in these competition experiments with $[\text{Mn}^{\text{II}}(\text{phen})_1]^{2+}$ were invariant over a 10-fold range of Mn concentrations, consistent with a mononuclear active oxidant (Table 4, entries 2–4).

Catalyst Recycling. With careful control of the reaction conditions, $\text{Mn}^{\text{II}}\text{T}$ is a durable, reusable catalyst. Under the conditions noted in Table 1, a sample of $\text{Mn}^{\text{II}}\text{T}$ was reused five times without a significant change in the manganese content in the materials, in the epoxide yields, and in the required amount of oxidant. Efficient control of the heat of the reaction was necessary to ensure that manganese did not leach from $\text{Mn}^{\text{II}}\text{T}$, which reduced the catalyst efficiency in subsequent runs. The recycling behavior of the $\text{Mn}^{\text{II}}\text{T}$ materials with ligand loadings of 0.33 and $0.13 \text{ mmol g}^{-1} \mathbf{1}^{\text{C}}$ were similar (Table 5). In contrast, $\text{Mn}^{\text{II}}\text{G}$ suffered from significant loss of reactivity and metal leaching upon reuse (Table 5), and consecutive reactions required longer times to reach completion at compa-

table manganese loadings. Even with the extended reaction time, the epoxide yields with $\text{Mn}^{\text{II}}\text{G}$ were lower. ICP analysis of the used catalysts, both $\text{Mn}^{\text{II}}\text{G}$ and $\text{Mn}^{\text{II}}\text{T}$, showed no significant loss in the sulfur content, and reloading of the used catalysts with $[\text{Mn}(\text{CF}_3\text{SO}_3)_2]$ reestablished their original reactivity.

Discussion

SBA-15 silica materials are attractive as supports for oxidation catalysts as the materials are readily synthesized and are oxidatively stable. The large surface area ($>600 \text{ m}^2 \text{ g}^{-1}$) and large average pore diameter ($>50 \text{ \AA}$) of these materials also provide for potential site isolation of covalently attached catalysts and facile diffusion of reagents and products, respectively. Our previous work with non-heme manganese epoxidation catalysts identified $[\text{Mn}(\text{II})(1,10\text{-phenanthroline})_2]^{2+}$ as a very active catalyst for a wide range of electron-deficient olefins using peracetic acid as an oxidant. A metal-template/metal-exchange procedure was developed to create bis(1,10-phenanthroline) metal coordination sites on the SBA-15 surface. The metal template was a stable 2:1 complex of ethyl 4-(3-(triethoxysilyl)propylthio)-1,10-phenanthroline-3-carboxylate ($\mathbf{1}^{\text{H}}$) with Cu(I), $[\text{Cu}^{\text{I}}(\mathbf{1}^{\text{H}})_2]^+$, and was initially formed in solution and subsequently attached to the silica to give $[\text{Cu}^{\text{I}}(\mathbf{1}^{\text{C}})_2]^+$ (Scheme 2). This four-coordinate, tetrahedral Cu(I) complex exists as a single diastereomer with the nonsymmetric $\mathbf{1}^{\text{H}}$ ligand. By contrast, a metal with a hexacoordinate tendency such as Mn(II) would almost certainly create a diastereomeric mixture of metal complexes, leading potentially to an increased heterogeneity of the templated sites. Another advantageous property of the copper is its substitution lability. Copper is removed readily with an appropriate chelating agent.^{44,45} Metalation of the material with manganese completes the metal-template/metal-exchange procedure.

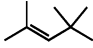
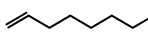
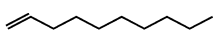
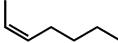
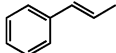
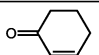
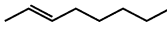
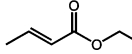
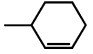
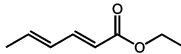
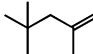
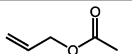
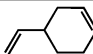
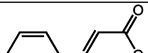

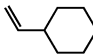
As measured by the pore size and surface area, the SBA-15 materials were not altered significantly by either the metal-template/metal-exchange procedure or the aggressive epoxidation reaction conditions used herein. Lower ligand loadings by this template procedure ($<0.3 \text{ mmol g}^{-1} \mathbf{1}^{\text{C}}$) resulted in more efficient and selective manganese catalysts, presumably because of the greater site isolation of the templated sites allowing for a greater homogeneity of formed manganese complexes. The metal-templated materials yielded consistently 2:1 $\mathbf{1}^{\text{C}}$ /metal ratios upon metal reloading with a variety of divalent metal ions (Fe, Mn, Cu). This coincides with the imprinted bis- $\mathbf{1}^{\text{C}}$ coordination environment from $[\text{Cu}^{\text{I}}(\mathbf{1}^{\text{C}})_2]^+$, which is retained upon metal exchange. Random grafting of the free ligand at low loadings exhibited $\mathbf{1}^{\text{C}}$ /metal ratio less than 2:1 after metalation with either Mn^{II} or Cu^{II} . Such low ratios are consistent with a distribution of bis- $\mathbf{1}^{\text{C}}$ and mono- $\mathbf{1}^{\text{C}}$ ligated metals.

X-band EPR analysis of the Cu^{II} complexes provided a sensitive probe into the environments of ligated Cu(II) in the templated ($\text{Cu}^{\text{II}}\text{T}$) and randomly grafted ($\text{Cu}^{\text{II}}\text{G}$) materials. The axial EPR spectra of both copper-loaded materials at 0.1 mmol g^{-1} of $\mathbf{1}^{\text{C}}$ is consistent with on-average site isolation, as tight packing of copper complexes would result in broad isotropic

(44) Smith, R. M.; Martell, A. E. *Critical Stability Constants*; Plenum Press: New York, 1975; Vol. 2.

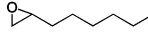
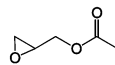
(45) Dietrich-Buchecker, C. O.; Sauvage, J. P.; Kern, J. M. *J. Am. Chem. Soc.* **1984**, *106*, 3043–3045.

Table 3. Epoxidation Activity of $\text{Mn}^{\text{II}}\text{T}$ ^a and $[\text{Mn}^{\text{II}}(\mathbf{2})_2]^{2+}$ ^b

Entry	Substrate	Catalyst	Yield (%)	Selectivity (%)	Entry	Substrate	Catalyst	Yield (%)	Selectivity (%)
1		$\text{Mn}^{\text{II}}\text{T}$	>99	>99	9		$\text{Mn}^{\text{II}}\text{T}$	90	95
		$\text{Mn}^{\text{II}}\text{G}$	90	90			$[\text{Mn}^{\text{II}}(\mathbf{2})_2]^{2+}$	85	85
		$[\text{Mn}^{\text{II}}(\mathbf{2})_2]^{2+}$	0	0	10		$\text{Mn}^{\text{II}}\text{T}$	90	90
		$[\text{Mn}^{\text{II}}(\mathbf{2})_2]^{2+}$	75	75					
2		$\text{Mn}^{\text{II}}\text{T}$	98 ^c	98	11		$\text{Mn}^{\text{II}}\text{T}$	>99	>99
		$\text{Mn}^{\text{II}}\text{G}$	95 ^d	95			$[\text{Mn}^{\text{II}}(\mathbf{2})_2]^{2+}$	95	95
		$[\text{Mn}^{\text{II}}(\mathbf{2})_2]^{2+}$	80 ^d	85	12		$\text{Mn}^{\text{II}}\text{T}$	>99	>99
		$[\text{Mn}^{\text{II}}(\mathbf{2})_2]^{2+}$	60	90					
3		$\text{Mn}^{\text{II}}\text{T}$	>99	>99	13		$\text{Mn}^{\text{II}}\text{T}$	98 ^e	98
		$[\text{Mn}^{\text{II}}(\mathbf{2})_2]^{2+}$	70	85			$[\text{Mn}^{\text{II}}(\mathbf{2})_2]^{2+}$	30 ^e	50
4		$\text{Mn}^{\text{II}}\text{T}$	95	>99	14		$\text{Mn}^{\text{II}}\text{T}$	>99 ^f	>99
		$[\text{Mn}^{\text{II}}(\mathbf{2})_2]^{2+}$	90	90			$[\text{Mn}^{\text{II}}(\mathbf{2})_2]^{2+}$	50 ^g	95
5		$\text{Mn}^{\text{II}}\text{T}$	95	95	15		$\text{Mn}^{\text{II}}\text{T}$	>99	>99
		$[\text{Mn}^{\text{II}}(\mathbf{2})_2]^{2+}$	85	85			$[\text{Mn}^{\text{II}}(\mathbf{2})_2]^{2+}$	80	80
6		$\text{Mn}^{\text{II}}\text{T}$	75 ^h	75	16		$\text{Mn}^{\text{II}}\text{T}$	90 ^{ij}	98
		$[\text{Mn}^{\text{II}}(\mathbf{2})_2]^{2+}$	65 ^h	65			$[\text{Mn}^{\text{II}}(\mathbf{2})_2]^{2+}$	50 ⁱ	80
7		$\text{Mn}^{\text{II}}\text{T}$	80 ^h	80					
		$[\text{Mn}^{\text{II}}(\mathbf{2})_2]^{2+}$	30 ^h	30					
8		$\text{Mn}^{\text{II}}\text{T}$	98	98					
		$[\text{Mn}^{\text{II}}(\mathbf{2})_2]^{2+}$	75	85					

^a 0.1 mmol g⁻¹ **1**^c, 0.5 mol % Mn, 1.5 equiv of PAA, 0.4 M substrate, 2 °C, 10 min, MeCN. ^b 0.5 mol % Mn, 1.8 equiv of PAA, 0.4 M substrate, 2 °C, 10 min, MeCN. ^c No appreciable *trans* epoxide product was detectable by GC or GC/MS. ^d GC and GC/MS showed ca. 5% *trans* epoxide. ^e 2.8 equiv of PAA were added for full conversion. ^f 3.0 equiv of PAA gave 98% diepoxide product. ^g 4.4 equiv of PAA yielded 55% 4,5-monoepoxide and 45% diepoxide after 30 min. ^h Yield indicates the diepoxide product with 2.8 equiv of PAA. ⁱ 1.8 equiv of PAA were required for full conversion. ^j Isolated yield of 80%.

Table 4. Chemoselectivity of Mn^{II} Catalysts in Intermolecular Competition Experiments^a

Entry	Catalyst	Product Ratio ^b	
			
1	$[\text{Mn}^{\text{II}}(\text{phen})_2]^{2+}$ ^c	12 (±1)	: 1
2	$[\text{Mn}^{\text{II}}(\text{phen})_1]^{2+}$ ^c [3.5 mM Mn]	9 (±1)	: 1
3	$[\text{Mn}^{\text{II}}(\text{phen})_1]^{2+}$ ^c [1.5 mM Mn]	9 (±1)	: 1
4	$[\text{Mn}^{\text{II}}(\text{phen})_1]^{2+}$ ^c [0.35 mM Mn]	9 (±1)	: 1
5	$[\text{Mn}^{\text{II}}(\mathbf{2})_2]^{2+}$ ^c	12 (±1)	: 1
6	$[\text{Mn}^{\text{II}}(\mathbf{2})_1]^{2+}$ ^c	10 (±1)	: 1
7	$\text{Mn}^{\text{II}}\text{T}$ (0.11 mmol g ⁻¹ 1 ^c)	7 (±1)	: 1
8	$\text{Mn}^{\text{II}}\text{T}$ (0.025 mmol g ⁻¹ 1 ^c)	7 (±1)	: 1
9	$\text{Mn}^{\text{II}}\text{G}$ (0.90 mmol g ⁻¹ 1 ^c)	10 (±1)	: 1
10	$\text{Mn}^{\text{II}}\text{G}$ (0.11 mmol g ⁻¹ 1 ^c)	7 (±1)	: 1
11	$\text{Mn}^{\text{II}}\text{G}$ (0.025 mmol g ⁻¹ 1 ^c)	6 (±1)	: 1

^a Reaction conditions: 0.43 μmol Mn, 32 μmol of 1-octene, 64 μmol of allyl acetate, 18 μmol of PAA, 0.4 M olefin, 2 °C, MeCN. ^b Averaged over five reactions. ^c Generated in situ with the appropriate $[\text{Mn}^{\text{II}}(\text{CF}_3\text{SO}_3)_2]$ /ligand ratio.

signals. A more detailed comparison of the spectra suggests that the copper coordination in $\text{Cu}^{\text{II}}\text{T}$ more closely resembles the tetra-nitrogen environment of homogeneous $[\text{Cu}^{\text{II}}(\mathbf{2})_2]^{2+}$ than that in $\text{Cu}^{\text{II}}\text{G}$. The larger g_{\parallel} values (ca. 2.29) of $\text{Cu}^{\text{II}}\text{G}$ as compared to $\text{Cu}^{\text{II}}\text{T}$ (ca. 2.27) suggest an increase in the oxygen atom ligation at the expense of nitrogen atom ligation.⁴⁶ Solution

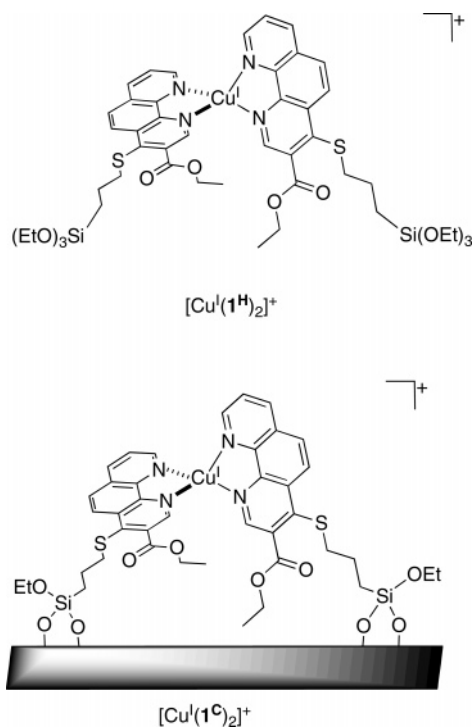
studies of $[\text{Cu}^{\text{II}}(\text{bpy})_2]^{2+}$ (bpy = bipyridine) show clearly that exchange of the dinitrogen bpy chelate for oxygen ligand(s) such as oxalate⁴⁸ or water yields larger g_{\parallel} values (Table 6).⁴⁹

(46) Peisach, J.; Blumberg, W. E. *Arch. Biochem. Biophys.* **1974**, *165*, 691–708.

Table 5. Recycling Trials: Mn Concentration and Epoxide Yield of Mn^{II}T and Mn^{II}G Materials^a

trial	Mn ^{II} T 0.33 1 ^c (mmol g ⁻¹)		Mn ^{II} T 0.13 1 ^c (mmol g ⁻¹)		Mn ^{II} G 0.090 1 ^c (mmol g ⁻¹)	
	Mn (mmol g ⁻¹) ^b	yield (%)	Mn (mmol g ⁻¹) ^b	yield (%)	Mn (mmol g ⁻¹) ^b	yield (%)
0	0.16		0.075		0.075	
1	0.16	96	0.075	96	0.065	75
2	0.15	96	0.075	96	0.060	70
3	0.15	96	0.066	96	0.030	65
4	0.14	94	0.061	96		
5	0.15	96				

^a 0.5 mol % Mn, 1.5 equiv of PAA, 0.4 M vinylcyclohexane, 2 °C, 10 min, MeCN. ^b ICP analysis.

Scheme 2

The residual silica silanol groups, with a pK_a near that of a carboxylic acid (~ 5),⁴⁷ are potential oxygen ligands, though water is also possible.

The addition of (*n*-Bu₄N)Cl to Cu^{II}G (2 equiv/Cu(II)) significantly alters the EPR spectrum with the appearance of multiple features in the $g_{||}$ region. Such behavior is consistent with variable ligation of chloride to copper yielding a heterogeneous distribution of copper sites. Similar titrations with Cu^{II}T at comparable ligand loadings only resulted in a slight shifting of the $g_{||}$ signals to a lower field. The copper coordination appears to remain homogeneous with well-formed bis-phenanthroline coordination.

Beyond the metal/ligand ratios and Cu^{II} EPR studies, the catalytic epoxide yields and substrate chemoselectivity further support a predominance of bis-1^c Mn^{II} species in Mn^{II}T and mono-1^c Mn^{II} species in Mn^{II}G. Reactivity of the homogeneous Mn^{II} catalysts, [Mn^{II}(phen)_{*n*}]²⁺, and [Mn^{II}(2)_{*n*}]²⁺ (*n* = 1 or 2) reveals that two coordinated 1,10-phenanthroline ligands are

Table 6. X-Band EPR Parameters of Some Cu^{II} Complexes^a

complex	$g_{ }$	g_{\perp}	g_{\perp}	$A (10^{-4} \text{ cm}^{-1})$	ref
[Cu ^{II} (2) ₂] ²⁺	2.270	2.065	2.055	160	herein
Cu ^{II} T ^b	2.267	2.060	2.060	155	herein
Cu ^{II} G ^b	2.295	2.060	2.060	155	herein
[Cu ^{II} (bpy) ₂] ²⁺	2.220	2.060	2.060	NA	48
[Cu ^{II} (bpy)(oxalate)]	2.228	2.126	2.066	NA	48
[Cu ^{II} (bpy)(OH ₂) ₂] ²⁺	2.315	2.072	2.072	166	49

^a NA = not available. ^b Materials with loadings of 0.1 mmol g⁻¹ 1^c are reported. Results are consistent with Cu^{II}G and Cu^{II}T materials with loadings from 0.3 to 0.03 mmol g⁻¹ 1^c.

optimal for epoxide product selectivity (Table 2). Not surprising is that Mn^{II}T materials maintain high reactivity and epoxide selectivity over a range of ligand loadings while Mn^{II}G materials exhibit a loss of epoxide selectivity as the ligand loading decreases. The electrophilic chemoselectivity of the homogeneous Mn^{II} catalysts varies with the number of coordinating ligands, as assessed through intermolecular competition experiments (Table 4). Mn^{II}T materials exhibit consistent chemoselectivity over a range of ligand loadings while Mn^{II}G materials vary with ligand loading. Immobilization and site isolation of a bis-1 coordination sphere confer a greater consistency in the epoxidation reactivity of the templated materials than is available from the homogeneous catalysts or the randomly grafted materials.

Very few electrophilic oxidants reported are as effective as Mn^{II}T/PAA at converting electron-deficient olefins in α,β -unsaturated ketones and esters to their corresponding epoxides, and yet Mn^{II}T/PAA is also able to convert electron-rich trisubstituted olefins to their respective epoxides in high yields. This latter result is striking given that [Mn^{II}(phen)₂]²⁺ with PAA in a homogeneous solution only degrades trisubstituted olefins to a variety of oxidized products, none of which is the epoxide. The lesser degree of isomerization determined with internal *cis*-olefins to *trans*-epoxide products with Mn^{II}T as compared to [Mn^{II}(phen)₂]²⁺ ($\sim 5\%$ *trans*-epoxide) suggests that surface immobilization reduces radical-like reactivity. Whether this is due to a reduced lifetime of a transition state with radical character or a reduction in the number and type of active manganese oxidant(s) in the materials is unknown.⁵⁰ The greater efficiency exhibited by Mn^{II}T as compared to [Mn^{II}(2)₂]²⁺ also emphasize the benefits of catalyst site isolation by precluding biomolecular catalyst deactivation processes. Mn^{II}T efficiently converts oxygen-functionalized olefins such as ethyl sorbate to the epoxide product (Table 3, entry 14) with only a slight excess of PAA, while [Mn^{II}(2)₂]²⁺ yields significantly less epoxide while requiring a greater amount of oxidant.

Recycling studies with Mn^{II}T confirm the robust nature of the bis-1^c templated materials. However, dropwise addition of freshly prepared PAA over 5 min is necessary to achieve high product yields, which ensures that the heat of the reaction is dissipated in the larger recycling runs. Reaction conditions that lead to manganese leaching from Mn^{II}T do not damage the covalently attached ligands, as reconstitution of this material to full manganese loading recovers full catalytic activity. Control experiments with unmodified material and Mn(CF₃SO₃)₂ show no measurable substrate conversion with α -olefins under the

(47) Rosenholm, J. M.; Czurykiewicz, T.; Kleitz, F.; Rosenholm, J. B.; Linden, M. *Langmuir* **2007**, *23*, 4315–4323.

(48) Walker, F. A.; Sigel, H.; McCormick, D. B. *Inorg. Chem.* **1972**, *11*, 2756–2763.

(49) Walker, F. A.; Sigel, H. *Inorg. Chem.* **1972**, *11*, 1162–1164.

(50) Another explanation of the *cis*-olefin isomerization difference between the Mn^{II}T and [Mn(phen)₂]²⁺ is different mechanisms of epoxidation. However, the similarity of the product distributions in the olefin competition experiments argues against such a postulate.

epoxidation reaction conditions used. Neither the production of epoxide nor the selectivity of the materials may be attributed to leaching metal.

Summary

We have developed a metal-template/metal-exchange method to control the distribution of covalently attached independent ligands in mesoporous silica at low loadings. Covalent attachment of a correlated distribution of closely positioned 1,10-phenanthroline ligands allows a bis-phen coordination to Mn^{II} to be achieved and maintained in the material at various ligand loadings. These imprinted manganese complexes are efficient and recyclable heterogeneous epoxidation catalysts using PAA and exhibit a greater substrate scope, more efficient oxidant use, and higher product selectivity than either its homogeneous or randomly grafted analogue. The correlated distribution of two 1,10-phenanthroline ligands is proposed to be critical to the consistent reactivity at various ligand loadings. Indeed, random grafting of the identical ligand allows the formation of competent catalysts, but the yield and the selectivity of the reaction are not as favorable and vary with ligand loading. The side reactions that occur with the homogeneous analogue leading to isomerization of *cis*-substrates and deactivation of the catalyst are attenuated significantly by covalent attachment and site isolation into the imprinted materials. Similar template processes may

prove beneficial for the immobilization of other catalysts that require multiple ligands in their coordination spheres and may provide access to coordination geometries not accessible in a homogeneous solution.

Acknowledgment. This work was supported by the NIH Grant GM-50730. The authors thank Dr. G. Li from the Soil and Environmental Biogeochemistry Department at Stanford for ICP analysis and Prof. E. I. Solomon for the EPR spectrometer use. The UCSF Mass Spectrometry Facility, supported by the Biomedical Technology Resource Centers Program of the National Center for Research Resources, NIH NCRR RR01614, provided the HRMS data.

Supporting Information Available: Surface area and pore diameter measurements of SBA-15 materials exposed to various reaction conditions are provided along with calculations of the estimated surface area coverage of a single tethered 1,10-phenanthroline ligand, $\mathbf{1}^{\text{C}}$, and the average surface area available on the material for various ligand loadings. EPR spectra of the Mn^{II} complexes and materials are also available. This material is available free of charge via the Internet at <http://pubs.acs.org>.

JA0742030